The Journal of Neuroscience, December 15, 2001, 21(24):9744–9756

Elevated Postsynaptic $[Ca^{2+}]_i$ and L-Type Calcium Channel Activity in Aged Hippocampal Neurons: Relationship to Impaired Synaptic Plasticity

Olivier Thibault, Robert Hadley, and Philip W. Landfield

Department of Molecular and Biomedical Pharmacology, MS-307 University of Kentucky College of Medicine, Lexington, Kentucky 40536-0298

Considerable evidence supports a Ca^{2+} dysregulation hypothesis of brain aging and Alzheimer's disease. However, it is still not known whether (1) intracellular $[Ca^{2+}]_i$ is altered in aged brain neurons during synaptically activated neuronal activity; (2) altered $[Ca^{2+}]_i$ is directly correlated with impaired neuronal plasticity; or (3) the previously observed age-related increase in L-type voltage-sensitive Ca^{2+} channel (L-VSCC) density in hippocampal neurons is sufficient to impair synaptic plasticity. Here, we used confocal microscopy to image $[Ca^{2+}]_i$ in single CA1 neurons in hippocampal slices of young-adult and aged rats during repetitive synaptic activation. Simultaneously, we recorded intracellular EPSP frequency facilitation (FF), a form of short-term synaptic plasticity that is impaired with aging and inversely correlated with cognitive function. Resting $[Ca^{2+}]_i$ did not differ clearly with age. Greater elevation of somatic $[Ca^{2+}]_i$ and greater depression of FF developed in aged neurons during 20 sec trains of 7 Hz synaptic activation, but only if the activation triggered repetitive action potentials for several seconds. Elevated $[Ca^{2+}]_i$ and FF also were negatively correlated in individual aged neurons. In addition, the selective L-VSCC agonist Bay K8644 increased the afterhyperpolarization and mimicked the depressive effects of aging on FF in young-adult neurons. Thus, during physiologically relevant firing patterns in aging neurons, postsynaptic Ca^{2+} elevation is closely associated with altered neuronal plasticity. Moreover, selectively increasing postsynaptic L-VSCC activity, as occurs in aging, negatively regulated a form of short-term plasticity that enhances synaptic throughput. Together, the results elucidate novel processes that may contribute to impaired cognitive function in aging.

Key words: frequency facilitation; imaging; homeostasis; dendrites; repetitive activation; memory

The calcium dysregulation hypothesis of brain aging and Alzheimer's disease, initially proposed in the mid-1980s (Khachaturian, 1984; Landfield and Pitler 1984; Michaelis et al., 1984, Peterson et al., 1985), suggests that aging alters brain Ca^{2+} regulation, resulting in impaired neuronal function and, eventually, neurodegeneration. In support of this view, substantial evidence has accumulated to show that multiple brain Ca^{2+} regulatory/Ca^{2+}-dependent processes change with aging (for review, see Gibson and Peterson, 1987; Khachaturian, 1989; Landfield et al., 1989; Disterhoft et al., 1993; Foster and Norris, 1997; Thibault et al., 1998; Verkhratsky and Toescu, 1998; Griffith et al., 2000). In hippocampal neurons in particular, several Ca^{2+}-dependent neuronal processes linked to learning and memory exhibit aging-related changes. These changes include an increase in the slow afterhyperpolarization (AHP) (Landfield and Pitler, 1984; Moyer et al., 1992; Disterhoft et al., 1996), reduced long-term potentiation (LTP) (Barnes, 1979, 1994; Moore et al., 1993; Shankar et al., 1998; Bach et al., 1999), enhanced long-term depression (LTD) (Norris et al., 1996, 1998), and impaired short-term frequency facilitation (FF) (Landfield et al., 1978, 1986; Ouanounou et al., 1999).

Received July 3, 2001; revised Sept. 24, 2001; accepted Sept. 26, 2001.

This work was supported in part by Grants AG04542 and AG10836 from the National Institute on Aging. We thank Drs. Thomas Foster and Nada Porter for helpful comments and Kelley Secrest for excellent assistance with this manuscript.

Correspondence should be addressed to O. Thibault, Department of Molecular and Biomedical Pharmacology, MS-307, University of Kentucky Medical Center, 800 Rose Street, Lexington, KY 40536-0298. E-mail: othibau@uky.edu.

However recent advances in single-cell imaging and simultaneous recording in slices (Miyakawa et al., 1992; Regehr and Tank, 1992; Perkel et al., 1993; Brown and Jaffe, 1994; Schiller et al., 1995; Magee and Johnston, 1997; Yuste et al., 1999) have been difficult to apply to the relatively opaque slices of adult/aged animals (Brown and Jaffe, 1994). Consequently, although a number of aging studies have examined neuronal Ca^{2+} content, only a few have imaged the intracellular Ca^{2+} concentration in single, functional brain neurons (Kirischuk and Verkhratsky, 1996; Murchison and Griffith, 1998) and none has done so during recording and synaptic activation (for review, see Thibault et al., 1998; Verkhratsky and Toescu, 1998). Thus, whether neuronal $[Ca^{2+}]_i$ regulation is altered with aging during physiologically relevant firing frequencies or whether such alteration is correlated with changes in plasticity remains uncertain.

In addition, the possible sources of altered Ca^{2+} regulation are not well understood. Voltage-dependent Ca^{2+} currents and potentials are enhanced in hippocampal CA1 neurons of aged rats (Landfield and Pitler, 1984; Kerr et al., 1989; Campbell et al., 1996) and rabbits (Moyer et al., 1992; Disterhoft et al., 1993), apparently mediated by an increase in the membrane density of L-type voltage-sensitive Ca^{2+} channels (L-VSCCs) (Thibault and Landfield, 1996). In addition, selective L-VSCC antagonists and other Ca^{2+} blockers can counteract the effects of aging on several aspects of neuronal and/or behavioral function, implying that L-VSCC activity may be necessary for the aging changes (Deyo et al., 1989; Landfield et al., 1989; Scriabine et al., 1989; Moyer et al., 1992; Norris et al., 1998; Shankar et al., 1998; Ouanounou et al., 1999). To date, however, there have been no

studies on the selective enhancement of L-VSCC activity, to test the key related question of whether increased L-VSCC activity is also sufficient to induce aging-like changes in function.

Here, we studied these unresolved questions using UV-compatible confocal laser scanning microscopy and simultaneous intracellular recording during repetitive synaptic stimulation at physiological frequencies. We chose to study $[Ca^{2+}]_i$ responses in relation to FF (the growth of synaptic responses during repetitive synaptic stimulation at 5–15 Hz), a prominent form of hippocampal short-term synaptic plasticity that modulates synaptic throughput (Andersen and Lomo, 1970). FF appears advantageous for such studies, because it is likely associated with dynamic $[Ca^{2+}]_i$ responses and may be sensitive to postsynaptic Ca^{2+} influx (Landfield et al., 1986). Moreover, FF is impaired with aging (Landfield et al., 1986; Ouanounou et al., 1999), inversely correlated with cognitive function (Landfield, 1988), and may play an important role in the deficient LTP seen with perithreshold stimulation in the aged hippocampus (Rosenzweig et al., 1997).

MATERIALS AND METHODS

Slice preparation. All experiments were conducted in compliance with the institutional guidelines of the Animal Care and Use Committee at the University of Kentucky. Young-adult (3–5 months of age) and aged (24–27 months of age) male Fischer 344 rats were anesthetized in a CO_2 chamber before rapid decapitation. Brains were rapidly removed (<1 min) and transverse hippocampal slices (250–350 μm) were cut with a vibratome (TPI, St. Louis, MO) into a cold oxygenated artificial CSF (ACSF) solution of the following composition (in mM): 128 NaCl, 1.25 KH_2PO_4, 10 glucose, 26 $NaHCO_3$, 3 KCl, 2 $CaCl_2$, and 2 $MgCl_2$. Slices were placed in an interface-type chamber at room temperature (21–23°C) gassed with 95% O_2–5% CO_2 for at least 1 hr. For sharp-electrode recording and imaging studies, a single slice (250 μm) was transferred with a fire-polished Pasteur pipette into a recording chamber (RC-22C; Warner Instruments, Co., Hamden, CT) perfused (1.5 ml/min) with oxygenated ACSF solution at 21–23°C (~305 mOsm). The recording chamber sat on the stage of an inverted Nikon microscope (Diaphot 300; Nikon Inc., Melville, NY) interfaced with a UV-compatible confocal laser scanning microscope (see below). For patch-clamp experiments, slices (350 μm) were placed in a recording chamber mounted on the stage of an upright microscope (E600FN; Nikon). Oxygenated ACSF was gravity-fed and delivered at 1.5 ml/min into the recording chamber. Controls were set (model TC^2 Bip; Cell Micro Controls, Norfolk, VA) such that ACSF was 32°C at the recording chamber input. For both sharp-electrode and patch-clamp recording experiments, electrode solutions were sterile-filtered (0.2 μm) and the ACSF was continually suctioned to maintain a constant flow and level in the recording chamber.

Electrophysiology. In the Ca^{2+} imaging/aging study, sharp microelectrodes were used for intracellular recording and indicator delivery and to minimally perturb the Ca^{2+} regulatory physiological properties of the internal milieu. However, in studies aimed at testing the effects of selectively enhancing membrane L-VSCC activity with the agonist Bay K8644, holding the intracellular environment constant appeared advantageous; therefore, whole-cell patch-clamp methods were used. Sharp microelectrodes (World Precision Instruments, Sarasota, FL) were pulled on a P80 puller (Sutter Instruments Co., Novato, CA) and had resistances of 100–150 MΩ when filled. Electrode tips were first filled at the tip by capillary action with 15 mM Indo-1or 20 mM Calcium Orange (Molecular Probes, Eugene, OR) in 150 mM $KmeSO_4$ (ICN Biomedicals Inc., Aurora, OH) and 10 mM HEPES. The rest of the electrode was then backfilled with 2 M $KmeSO_4$ (ICN Biomedicals Inc.) in 40 mM HEPES. Somata of CA1 neurons were impaled and recordings were obtained in current-clamp mode with bridge-balance neutralization (Axoclamp 2A amplifier; Axon Instruments Inc., Union City, CA). Voltage signals were sampled at 1–3 kHz.

Patch-clamp electrodes were pulled from Fisher Scientific (Houston, TX) micro-hematocrit glass capillaries (# 02-668-68) on a Sutter Instruments pipette puller. Electrodes were coated with polystyrene Q-dope (GC Electronics, Rockford, IL) and had resistances of 2.9–3.7 MΩ in the bath. Pipettes were filled with the following solution (in mM): 140 $KmeSO_4$, 10 HEPES, 14 Tris-phosphocreatine, 4 Tris-ATP, and 0.3 Tris-GTP. The osmolarity of the solution was ~300 mOsm and the pH was adjusted to 7.3 with Trizma Base (Sigma, St. Louis, MO). Small steps (~1 μm) were used in combination with slight positive pressure to move the electrode into the stratum pyramidale until a GΩ seal was formed on the soma of a cell; the whole-cell patch-clamp recording configuration was then established in voltage-clamp mode (Blanton et al., 1989). After break-in, neurons were held at −70 mV for ~5 min to allow membrane sealing and stabilization; measures of capacitance and input resistance were then obtained with small hyperpolarizing steps. The remainder of the experiment was conducted in current-clamp mode (Axoclamp 1D; Axon Instruments) with bridge balance and electrode capacitance neutralization. Voltage records were digitized at 2–20 kHz and low-pass-filtered at 2 kHz.

Synaptic stimulation and frequency facilitation. In all experiments, a twisted bipolar stainless-steel stimulation electrode (0.0045 inches, coated; A-M Systems, Inc., Everett, WA), was positioned in the Schaffer collaterals/commissural fibers of the stratum radiatum, ~500 μm from the recorded neuron, to deliver synaptic stimulation. Input–output relationships were determined in every cell during synaptic stimulation (0.1 msec pulses) at 0.2 Hz. In sharp-electrode studies (imaging), the stimulus intensity for the subthreshold stimulation protocol was set to a level that generated a 4–5 mV baseline EPSP. For the suprathreshold stimulation protocol, stimulation current intensity was set 50% above the Na^+ action potential threshold to ensure consistent action potential generation in all cells. In the patch-clamp studies (Bay K8644), subthreshold FF was induced with a protocol similar to that described above, but in the suprathreshold protocol, intensity was set just at action potential threshold. The latter protocol was used to determine whether any effects of Bay K8644 on EPSP facilitation also affected action potential generation. Stimulation was delivered with an SD9K stimulator (Astro Med Inc., Grass Instruments, Warwick, RI).

The frequency facilitation of the EPSP was assessed during two sequential 20 sec trains of 7 Hz of synaptic stimulation at suprathreshold and subthreshold intensity, in cells with membrane potential initially set at −70 mV in current clamp. To avoid confounding by other, longer forms of plasticity or by declining "health," the second train was run only in neurons in which EPSP amplitude and resting $[Ca^{2+}]_i$ returned to baseline values within 5–10 min after the first train. Facilitation was measured as the percentage of change in the amplitude of each of 139 consecutive EPSPs relative to the baseline EPSP (the first EPSP of the 20 sec, 7 Hz train of stimulation), using Synaptosoft mini analysis (Synaptosoft Inc., Decatur, GA). The percentage of facilitation was averaged across 1 sec segments for statistical analyses (Fig. 1*C*). In suprathreshold protocols, the amplitude of the EPSP was measured at the inflection point between the action potential and the EPSP on the back downstroke of the Na^+ spike. Confirmation that this method accurately measured EPSP amplitude was obtained from measures of EPSPs in instances in which the action potential failed (Fig. 2), which showed that both approaches yielded highly similar values. For correlational analyses with imaging, FF was measured as the mean EPSP amplitude during the first 2 sec of the stimulus train (FF_{early}, first 13 EPSPs after the baseline EPSP), coinciding with a 2 sec imaging window (see below), and the last 2 sec of the train (FF_{late}, last 14 EPSPs), coinciding with the last 2 sec imaging window.

Mechanisms of frequency facilitation and hyperpolarizing/depolarizing shifts. Multiple processes interact during repetitive synaptic activation. As do most forms of short-term synaptic plasticity (Magleby, 1987; Zucker, 1996; Kreitzer et al., 2000), hippocampal FF (also termed "frequency potentiation") (Andersen and Lomo, 1970) appears to depend primarily on presynaptic mechanisms (Andersen and Lomo, 1970; Creager et al., 1980; Applegate and Landfield, 1988). Notably, hippocampal FF is associated with massive presynaptic vesicle mobilization to active zones (Applegate and Landfield, 1988), consistent with enhanced release probability and a presynaptic mechanism (Rosenmund and Stevens, 1996). Nevertheless, postsynaptic factors can modify short-term plasticity. For example, paired-pulse facilitation can be enhanced by postsynaptic IPSP suppression (Davies and Collingridge, 1996). It also has been suggested that suppression of $GABA_A$-mediated postsynaptic inhibition during prolonged repetitive activation in the hippocampus may contribute to facilitation (McCarren and Alger, 1985). However, this seems unlikely, because the $GABA_A$ antagonist bicuculline does not alter FF (Pitler and Landfield, 1987). In addition, the onset of synaptically induced FF in the hippocampus is accompanied by a substantial postsynaptic hyperpolarization and membrane conductance increase (Landfield et al., 1986; Pitler and Landfield, 1987) that appears to be a combination

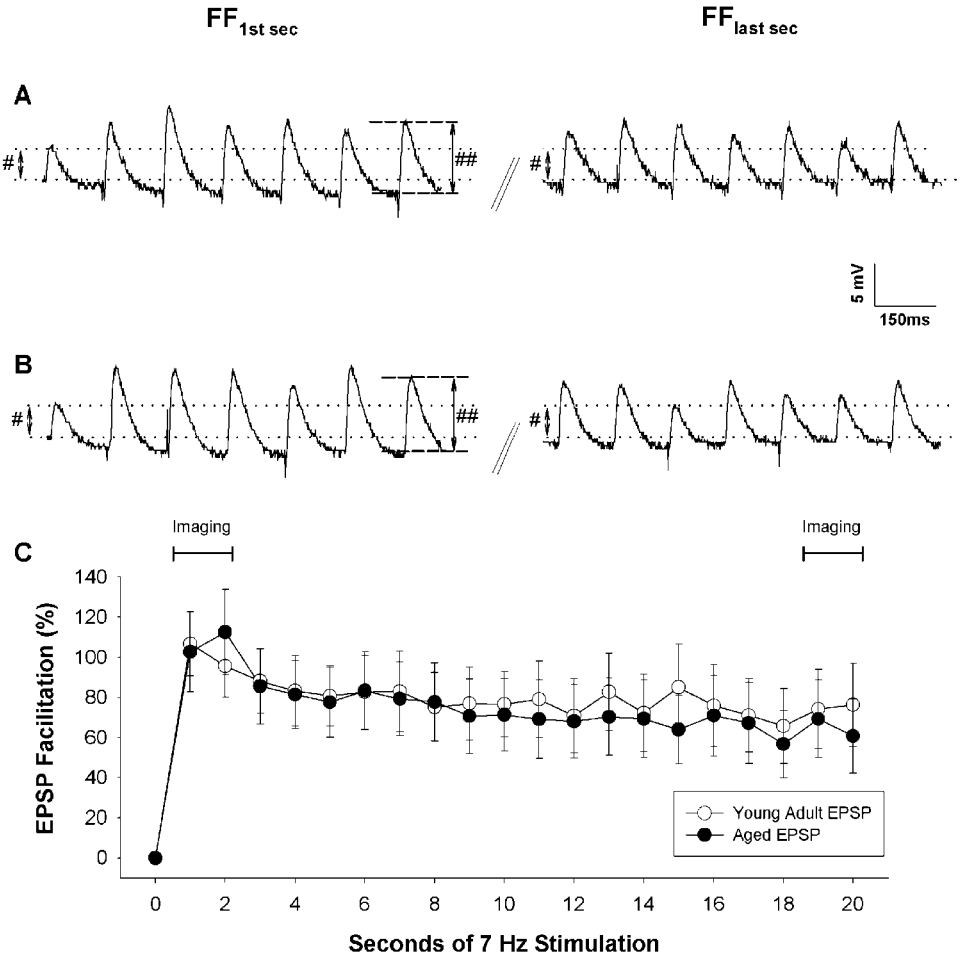

Figure 1. Subthreshold frequency facilitation. Representative intracellular voltage traces recorded in a young-adult (*A*) and an aged (*B*) CA1 neuron during 7 Hz of synaptic activation below threshold for a Na^+ action potential. The first second (*left*) and the last second (*right*) of a 20 sec train of repetitive activation are shown. The first EPSP of the first second record is the baseline EPSP. The baseline EPSP (*arrow*, #) is delimited by two *dotted lines*, extended across the width of the figure to highlight the degree of facilitation during the 20 sec train. Measurement of EPSP facilitation during the train is illustrated by the second *arrow* (##) and two *dashed lines*. An initial hyperpolarization accompanies repetitive activation but partly decays with EPSP facilitation by the end of the train (see Materials and Methods). Note that EPSPs during the train are measured from the hyperpolarized membrane potential. *C*, Mean ± SEM of the percentage of facilitation averaged in 1 sec segments during the 20 sec train ($n = 11$ young-adult and 11 aged neurons). No significant differences were seen between the two age groups. For simultaneous imaging in the same cells, Ca^{2+} transients were acquired during the first 2 sec and the last 2 sec of the simulation train (*horizontal bar insets*).

of a late IPSP (Newberry and Nicoll, 1984) and the Ca^{2+}-dependent AHP (Madison and Nicoll, 1984; Storm, 1990). After a few seconds of repetitive stimulation above but not below spike threshold, this ongoing hyperpolarization converts to depolarization. This depolarizing shift appears to be mediated by a large K^+ efflux via spike-triggered AHP and delayed rectifier conductances, with a resulting accumulation of extracellular K^+ and a shift in the K^+ equilibrium potential (Alger and Teyler, 1978; Creager et al., 1980; Pitler and Landfield, 1987). After additional seconds of activation, the membrane exhibits hyperpolarization again (apparently mediated by Na^+/K^+ pump activation), which then decays roughly along with the decay of EPSP facilitation. Unless extreme, these fluctuations in membrane potential, although briefly affecting spike probability (Alger and Teyler, 1978; Creager et al., 1980; Pitler and Landfield, 1987), have little effect on EPSP magnitude. However, the increased membrane conductance that accompanies both the hyperpolarization and depolarization phases can shunt EPSP amplitude (Pitler and Landfield, 1987).

Studies with Bay K8644. A 1 mM stock solution of Bay K8644 in DMSO was delivered at the mouth of the perfusion chamber via a cannula and tubing attached to a syringe perfusion pump (model 341B; Sage Instruments, Cambridge, MA). The perfusion rate of the syringe was 1000-fold slower than the main perfusate, providing a final concentration of 1 μM Bay K8644 in 0.1% DMSO. Control slices were perfused with 0.1% DMSO. The AHP was triggered from a set membrane potential of −60 mV, using a 150 msec intracellular depolarizing current pulse sufficient to generate three to four Na^+ action potentials. AHPs were elicited every 30 sec and AHP amplitudes were measured 750 msec after the end of each pulse. AHP amplitudes were derived by averaging at least three consecutive AHP measures obtained in the baseline period and after 15 min of drug or vehicle. For each cell studied for AHP amplitude, the same number of Na^+ action potentials was carefully maintained from the start of the experiment throughout its duration (15 min of Bay K8644 or vehicle) by small adjustments of injected current intensities. Synaptic activation protocols were then performed as described above.

$[Ca^{2+}]_i$ Imaging. Imaging studies were performed on a real-time (30 Hz), inverted confocal laser scanning microscope (RCM 8000; Nikon Inc.) equipped with a 40× water immersion objective. For ratiometric studies, the Ca^{2+} fluorophore Indo-1 was excited using an argon laser generating multiline UV light (351–364 nm). Ratiometric measures of $[Ca^{2+}]_i$ were derived from two images acquired simultaneously through a dichroic mirror centered at 445 nm ("400 nm" and "500 nm" images). Images were obtained by signal averaging 60 images across 2 sec periods. To reduce UV damage, 2 sec images were obtained only for the first 2 sec period (FF_{early}) and the last 2 sec period (FF_{late}) of the 20 sec 7 Hz train. Because of the confocal nature of the images, out-of-focus background fluorescence (from adjacent cells or processes of the same cell above or below the plane of focus) was minimal (Brown and Jaffe, 1994); nevertheless, all signals were background subtracted offline using an area near to the cell of interest. Metamorph software (Universal Imaging Corporation, West Chester, PA) was used to measure the average gray values of the region of interest (the entire somatic region or the proximal apical dendrite) in each cell.

Ratio values were calibrated to generate estimates of free Ca^{2+} using a standardized series of droplets containing 50 μM Indo-1 and seven increasing Ca^{2+} concentrations (0–39.8 μM free Ca^{2+},1 mM Mg^{2+}; Molecular Probes). The standard curve obtained from this *in vitro* calibration was fitted to yield several parameters: R_{min}, the minimum ratio in the absence of Ca^{2+}, R_{max}, the maximum ratio at saturating Ca^{2+} concentrations, K_d, the dissociation constant for Ca^{2+} binding to the indicator, and a constant (β) equal to the ratio of the 500 nm image in zero Ca^{2+} to the 500 nm image in 39.8 μM Ca^{2+}. The extracted values were 0.8 for R_{min}, 2.7 for R_{max}, and 565 for $K_d\beta$. Cell ratios were converted to free Ca^{2+} concentration ($[Ca^{2+}]_i$) using the following equation: $[Ca^{2+}]_i = K_d\beta\,(R - R_{min})/(R_{max} - R)$, in which R is the 400 nm/500 nm fluorescence emission ratio of the imaged cell (Grynkiewicz et al., 1985). *In situ* calibration by whole-cell patch or in nondissociated slice neurons is known to be problematic (Regehr and Tank, 1992). However, to cross-validate our *in vitro* calibration, we used *in situ* cali-

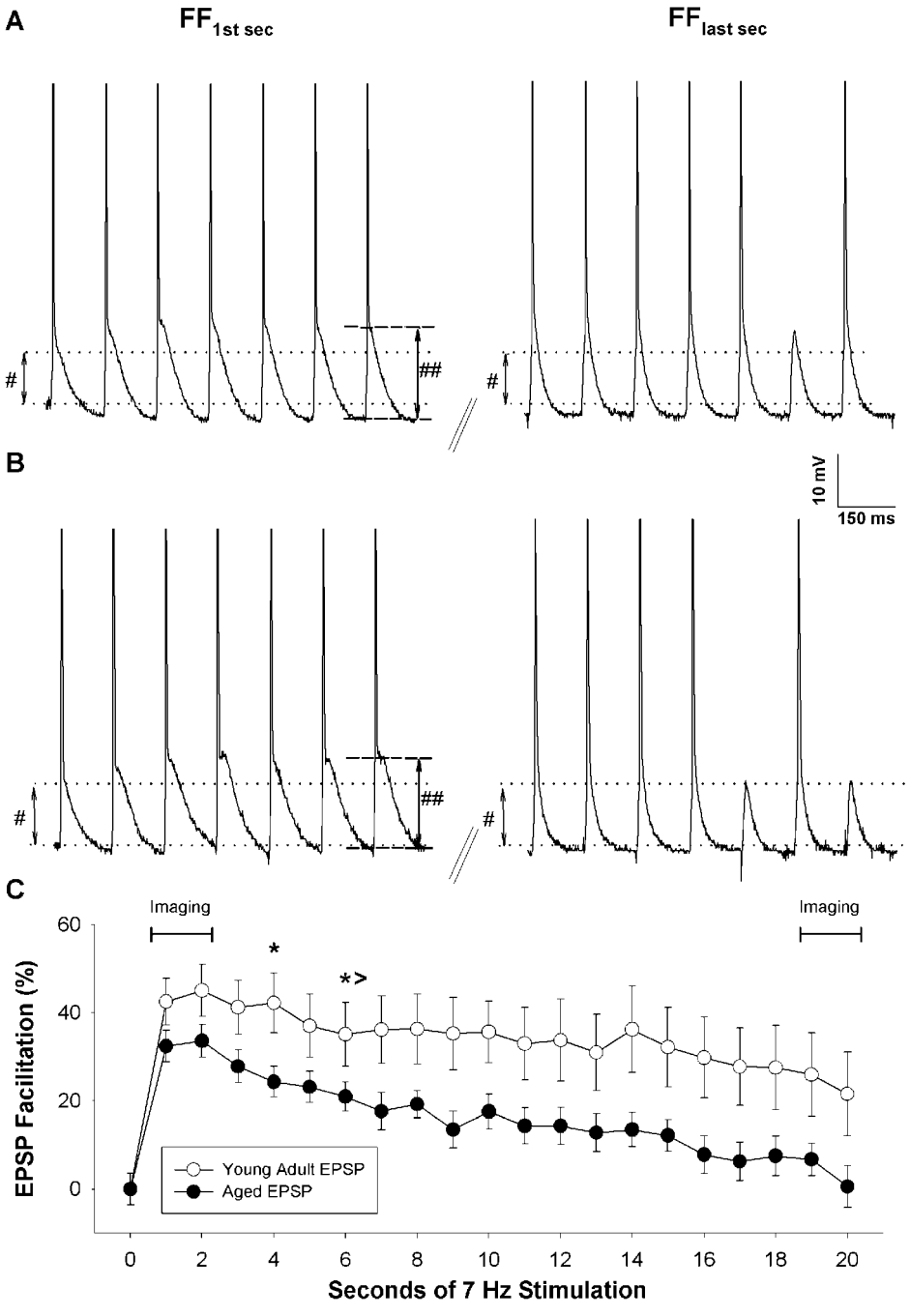

Figure 2. Suprathreshold frequency facilitation. Representative traces from a young-adult (*A*) and an aged (*B*) CA1 neuron during the first and last sec of 7 Hz of synaptic stimulation above threshold for a Na^+ action potential. In the young-adult neuron, the baseline EPSP (*#*, *dotted line*) was facilitated rapidly and then depressed slightly over the 20 sec train. In the aged neuron, the initial degree of facilitation (*##*, *dashed lines*) was similar, but the EPSP depressed nearly to baseline by the end of the stimulation train ($FF_{last\ sec}$). *C*, Mean ± SEM data (n = 15 young-adult and 16 aged neurons). *Significant age difference ($p < 0.05$); *> significant age difference at this point and all points thereafter. Imaging transients were acquired during the first 2 sec and the last 2 sec of the simulation train (*bar insets*). Action potentials are truncated for illustrative purposes.

bration in hippocampal neurons grown in culture (Porter et al., 1997). Neurons were loaded with a series of increasing Ca^{2+} concentrations and 50 μM Indo-1 using whole-cell patch pipettes. Five to eight cells per Ca^{2+} solution were imaged. In addition, to control for the possibility of aging differences in K_d, we also estimated $[Ca^{2+}]_i$ using different K_ds for young and aged cells, based on values published in a study comparing dissociated brain neurons from young-adult and aged animals (Murchison and Griffith, 1998). Analyses of Ca^{2+} data showed that the age-dependent $[Ca^{2+}]_i$ differences reported here were significant with any of these calibrations.

To image Ca^{2+} in dendritic segments and to obtain imaging data throughout the full stimulation train, we also used the single-wavelength Ca^{2+} indicator Calcium Orange. Compared with Indo-1, this indicator is excited and emits at longer wavelengths, improving tissue penetration, decreasing scatter, and improving resolution. Calcium Orange was excited using an He–Ne laser (543 nm), which is less likely to cause photodamage during repetitive imaging. Single images were acquired consecutively throughout the train in 2 sec windows and temporally synchronized to electrophysiological responses via TTL pulses. Relative Ca^{2+} changes during the stimulation were expressed as the percentage of change from baseline fluorescence ($\%\Delta F/F$). Images were obtained from different dendritic segments running from the base of the proximal apical dendrites to ~200 μm along the main apical dendrite. Metamorph software was used to measure average fluorescence in each segment. All signals were background subtracted from an area near the cell and were also corrected for bleaching.

Cell yield and selection criteria. An important issue in brain aging studies is the possibility that interactions between age and preparation procedures may preferentially damage aged neurons and introduce potential bias. Electrophysiological studies examining this question have found few age differences in resting potential, yield, input resistance, or action potential threshold and amplitude (Barnes and McNaughton, 1980; Landfield and Pitler, 1984; Kerr et al., 1989; Moyer et al., 1992; Disterhoft et al., 1993; Potier et al., 1993) (for review, see Barnes, 1994;

Table 1. Basic neuronal parameters in young-adult and aged CA1 neurons

	Young-adult (n = 15)	Aged (n = 16)
Input resistance (MΩ)	58.9 ± 3.7	61.9 ± 3.3
Resting membrane potential (mV)	−58.7 ± 1.1	−58.8 ± 1.3
Action potential threshold (μA)	151 ± 15	181 ± 15
Action potential amplitude (mV)	83.8 ± 1.3	81.9 ± 2.3
Action potential width at base (msec)	2.3 ± 0.2	2.4 ± 0.1
Action potentials during 20 sec train (n)	134.6 ± 8.4	126.9 ± 8.1
Action potentials during FF_{early} (n)	14 ± 0	14 ± 0
Action potentials during FF_{late} (n)	11.2 ± 1.3	10.2 ± 1.3
Interval, slicing to imaging (hr)	3.85 ± 0.4	4.3 ± 0.3

All values are mean ± SEM. No significant age-dependent differences were detected. Threshold was the synaptic stimulation electrode current necessary to trigger a Na^+ action potential. Action potential amplitude was measured from the peak of the EPSP. Action potential number values (n) were obtained during the 7 Hz suprathreshold train of synaptic activation.

Thibault and Landfield, 1996; Barnes et al., 1997). However, a recent study found that age may interact with brain slice procedures under some conditions (Moyer and Brown, 1998). Therefore this issue was assessed with specific regard to our imaging preparation.

Only cells held with minimal holding current (−0.05 to −0.3 nA), input resistances of >35 MΩ, overshooting action potentials, and no signs of hyperexcitability or abnormal depolarization during stimulation were included in the cell imaging analysis. Cells also were excluded if resting $[Ca^{2+}]_i$ was >200 nM. These criteria resulted in a comparable yield of recorded and imaged cells between young-adult and aged animals. In the young-adult slices, we recorded and imaged 15 neurons (from 13 animals) that met all criteria throughout the full suprathreshold protocol. In aged slices, we recorded and imaged 16 cells (from 13 animals) that met all criteria throughout the suprathreshold protocol. Eleven neurons of each age group also met all criteria through the subthreshold protocol. Overall, including neurons that met initial criteria and yielded resting $[Ca^{2+}]_i$ data but were not held throughout the full protocol, we recorded and imaged 39 neurons from 33 young-adult animals (approximate yield of 1.2) and 31 neurons from 24 aged animals (approximate yield of 1.3). Thus, our yield of healthy cells was at least as high in the aged group. For neurons run through the full protocol, there were no age differences in input resistance, resting potential, or action potential height, width, or threshold (Table 1). Moreover, there was no significant age difference in mean interval between slice preparation and cell imaging/recording (Table 1). There also was no significant correlation of the interval between the slice preparation and cell imaging with either resting or stimulated $[Ca^{2+}]_i$ in individual neurons (e.g., $r = 0.30$ for resting $[Ca^{2+}]_i$ and $r = 0.14$ for FF_{late} $[Ca^{2+}]_i$ in aged cells).

In addition, baseline fluorescence gray values at rest did not differ significantly with age for either the 400 or 500 nm images. In analyses of cells recorded through the full suprathreshold protocol or analyses of the larger set, including cells that were not held for the full protocol, we found no correlation between $[Ca^{2+}]_i$ (at rest or during stimulation) and distance from the edge of the slice. Thus, it appears unlikely that age differences in indicator loading or transmission through the tissue contributed to the age-dependent differences in estimated Ca^{2+}.

RESULTS

As noted above, most resting electrophysiologic measures recorded in CA1 neurons were unaffected by age (Table 1). However, the stimulus intensity needed to generate a threshold EPSP was modestly increased in the aged neurons (Table 1), likely because of decreased excitatory transmission (Barnes et al., 1997).

Frequency facilitation of the EPSP

Figure 1 illustrates the FF of the EPSP during subthreshold stimulation in a young-adult (Fig. 1*A*) and an aged (Fig. 1*B*) cell. FF develops rapidly and reaches maximal values within a few pulses. As noted above (see Materials and Methods), hyperpolarization also develops with the first few pulses, although it declines along with FF by the end of the 20 sec train (Fig 1. $FF_{last\ sec}$). For ease of comparison, the two central dotted lines and small arrows (Fig. 1, #) illustrate the amplitude of the first baseline EPSP, whereas the two outer dashed lines and large arrows (Fig. 1, ##, $FF_{first\ sec}$) illustrate measurement of the facilitated EPSP during repetitive stimulation. Note that the facilitated EPSP is measured from the hyperpolarized baseline. Facilitation was relatively well-maintained throughout the duration of the train in the subthreshold protocol, because EPSPs recorded during the last seconds of stimulation were still significantly facilitated (Fig. 1, $FF_{last\ sec}$). In 11 young-adult and 11 aged neurons with comparable baseline EPSP values (4.1 ± 0.3 and 4.2 ± 0.4 mV, respectively), no significant age-dependent difference was seen in the degree of facilitation measured during the duration of the stimulation (Fig. 1*C*). In addition, depression of FF from its maximal value at 1 sec was modest, and in both groups FF still exceeded 60% by the end of the train.

A different pattern was seen during the suprathreshold activation protocol. Figure 2 shows representative responses during synaptic activation above Na^+ action potential threshold in a young-adult (Fig. 2*A*) and an aged (Fig. 2*B*) cell. Baseline EPSP amplitudes for young-adult and aged neurons averaged 12.2 ± 0.8 and 12.2 ± 0.5 mV, respectively. In general, the percentage of amplitude facilitation was less in the suprathreshold compared with the subthreshold protocol. Moreover, in this protocol, aged neurons displayed a significant decline in FF relative to young-adult neurons (Fig. 2*C*, $n = 15$ young-adult and 16 aged neurons from 13 young-adult and 13 aged animals). Two-way ANOVAs (for repeated measures) of EPSP amplitude facilitation revealed a highly significant overall effect of stimulation ($p < 0.001$), as well as a significant main effect of age ($F_{(1,29)} = 4.8$; $p < 0.05$). *Post hoc* analyses indicated that the age difference developed starting after the fourth to fifth second of stimulation and was sustained thereafter. A similar effect was observed for EPSP area, which tended to decline more in aged cells (young-adult, +10.5 ± 18.9 vs aged, −13.8 ± 7.4 at FF_{late}). However, because of variability in EPSP width, this effect was not significant. Hyperpolarization also was present at the start of the suprathreshold train but, as noted above (see Materials and Methods), the synaptically activated hyperpolarization is a multicomponent and varying process that, unlike the AHP, does not clearly differ with age.

$[Ca^{2+}]_i$ Image quality

Older brain tissue is more opaque than the juvenile tissue generally used in imaging studies and, therefore, yields lower resolution images (Brown and Jaffe, 1994; Moyer and Brown, 1998). Moreover, because the question of whether absolute neuronal $[Ca^{2+}]_i$ levels are altered in aging was central to these studies, a ratiometric indicator was used to estimate $[Ca^{2+}]_i$. Like most ratiometric indicators, Indo-1 uses UV light that does not penetrate as readily through tissues as higher wavelengths. In addition, because large numbers of comparable samples with low variance must be obtained for statistical comparison in an aging study, we set the UV laser power at ~25% of its maximal output (also, to

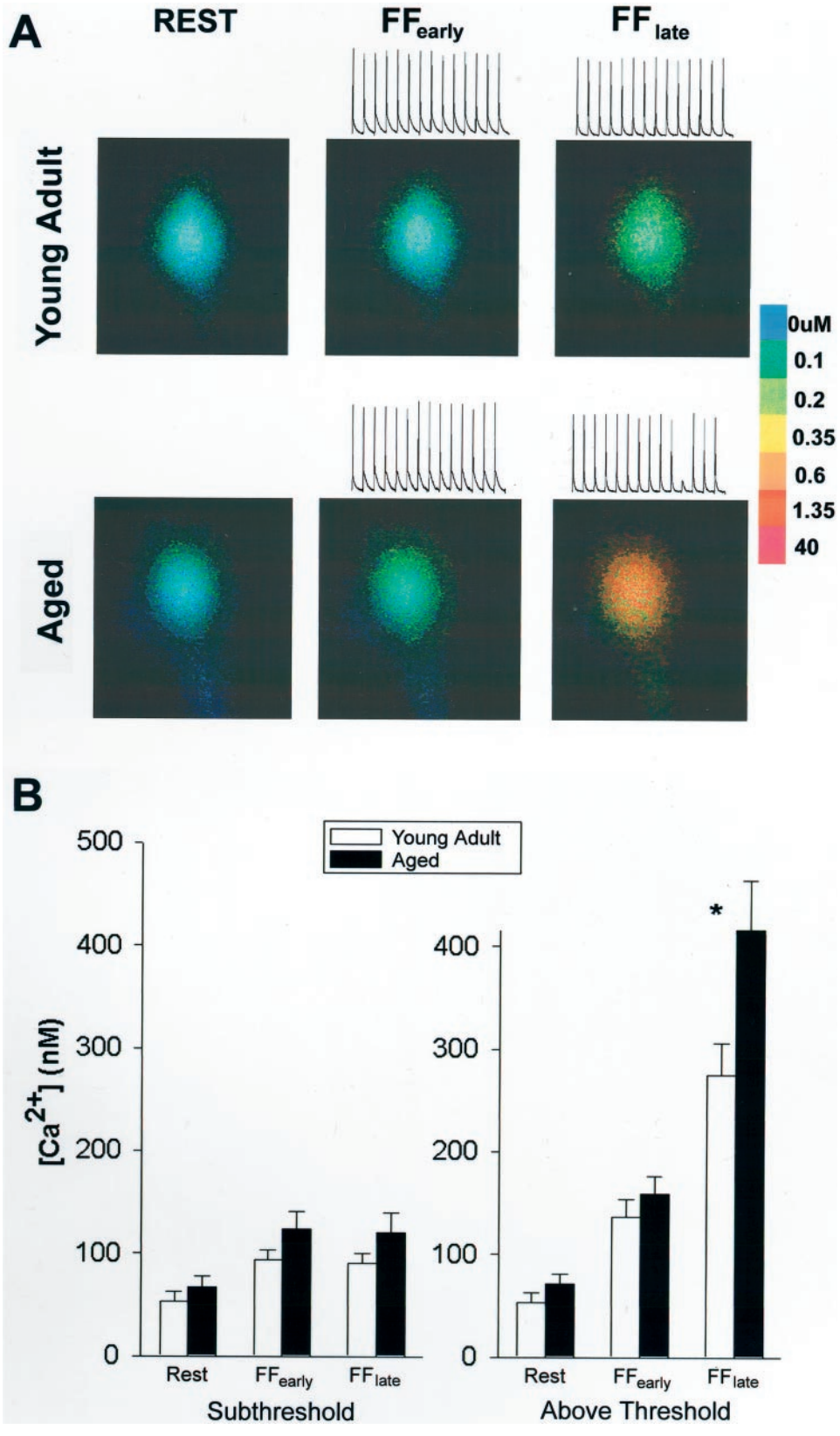

Figure 3. *A*, Representative pseudocolor Indo-1 ratiometric images acquired from the somata of a young-adult (*top*) and an aged (*bottom*) CA1 pyramidal neuron in hippocampal slices during repetitive suprathreshold stimulation. Images were acquired at rest (*left*), as well as during the first 2 sec of the 7 Hz stimulation (FF_{early}, *middle*) and the last 2 sec of stimulation (FF_{late}, *right*). Note the substantially greater elevation of $[Ca^{2+}]_i$ in the aged neuron (*A*, *bottom*) at FF_{late}. Electrophysiologic traces above each image are simultaneous current-clamp recordings from the same cells demonstrating comparable action potential generation and similar responses in the two cells. *B*, Mean ± SEM results for measures of $[Ca^{2+}]_i$ obtained at rest, during the first 2 sec, and during the last 2 sec of the 20 sec trains of the 7 Hz synaptic activation. *Left*, Same cells as shown in Figure 1*C*, studied during the subthreshold stimulation protocol ($n = 11$ per group). *Right*, Same cells shown in Figure 2*C* during the suprathreshold stimulation protocol ($n = 15$ young-adult and 16 aged neurons). Significant aging differences were found for $[Ca^{2+}]_i$ in the suprathreshold but not in the subthreshold protocol. $^*p < 0.05$ by ANOVA and *post hoc* analysis.

further minimize UV damage, images were acquired only at two time points, the first and last 2 sec periods of the 20 sec train). Because of these limitations, we imaged Indo-1 only in the somatic region of each cell, where a lower surface to volume ratio relative to dendrites significantly improves signal detection. Nevertheless, somal images were consistently bright (Fig. 3*A*) and these resolution issues should not influence the accuracy of ratiometric estimates of somal $[Ca^{2+}]_i$.

$[Ca^{2+}]_i$ before and during stimulation

Figure 3*A* illustrates representative $[Ca^{2+}]_i$ responses in a young-adult (top) and an aged (lower) CA1 neuron at the FF_{early} and FF_{late} periods during repetitive 7 Hz stimulation. The concomitant electrophysiologic traces from the same cells above each image show that comparable action potentials were generated in both cells throughout the train.

The mean resting $[Ca^{2+}]_i$ values acquired just before the onset of stimulation for the subset of neurons in which the full 20 sec suprathreshold protocol was completed (15 young-adult and 16 aged neurons) were 53.3 ± 9.5 and 71.4 ± 9.0 nM, respectively (Fig. 3*B*); these values did not differ statistically with age. Moreover, in the larger population of neurons for which resting values were obtained ($n = 39$ young-adult and 31 aged neurons), resting $[Ca^{2+}]_i$ also was not different with age (63.2 ± 8.0 nM for young-adult neurons and 75.1 ± 8.0 nM for aged neurons).

During repetitive subthreshold stimulation, $[Ca^{2+}]_i$ rose modestly in the first 2 sec in both young-adult and aged neurons and then remained relatively constant through the last 2 sec (FF_{late}). The small trend for $[Ca^{2+}]_i$ to be greater in aged neurons was not statistically significant (Fig. 3*B*, *left*). However, a very different pattern emerged during repetitive stimulation above action potential threshold. $[Ca^{2+}]_i$ rose substantially more in the FF_{early} period and continued to accumulate during the train such that $[Ca^{2+}]_i$ was greater at FF_{late} than at FF_{early}. Moreover, this latter effect was significantly greater in aged neurons (Fig. 3*B*, *right*). An ANOVA of FF_{early} and FF_{late} $[Ca^{2+}]_i$ transients revealed a significant aging-dependent difference in $[Ca^{2+}]_i$ during the stimulation train ($F_{(1,29)} = 5.3$; $p < 0.05$), and *post hoc* analyses (Tukey's test) showed that this was attributable primarily to age differences during FF_{late} ($p < 0.001$). Because of the clear enhancing effect of action potentials on $[Ca^{2+}]_i$ elevation (Miyakawa et al., 1992; Regehr and Tank, 1992; Brown and Jaffe, 1994; Schiller et al., 1995; Yuste et al., 1999), the number of action potentials was carefully monitored during each suprathreshold protocol. No age differences were found over the entire 20 sec train or during the first 2 sec or last 2 sec periods of the train that corresponded to the imaging windows (Table 1).

Negative correlation between somal $[Ca^{2+}]_i$ and facilitated EPSPs in aged neurons

The prediction of an inverse correlation between EPSP facilitation and elevated $[Ca^{2+}]_i$ was tested across individual young-adult and aged neurons. No significant correlation was seen in young-adult animals for suprathreshold FF_{late} ($r = +0.14$; $p = 0.25$) (Fig. 4*A*) or for either age group during FF_{early} or at either time point of the subthreshold protocol (data not shown). However, a significant negative correlation was found in aged neurons during the FF_{late} period of the suprathreshold protocol ($r = -0.54$; $p < 0.01$), regardless of whether absolute EPSP amplitude or FF percentage values were used (Fig. 4*B*). Thus, the inverse correlation between $[Ca^{2+}]_i$ and FF was seen only under conditions of repetitive action potential generation lasting several seconds and only in the age group exhibiting the greatest elevation of $[Ca^{2+}]_i$ (aged, suprathreshold, FF_{late}).

Dendritic and somal imaging throughout the train

Because only the first and last 2 sec periods during the 20 sec train were imaged in the Indo-1 study, it was not clear how closely the $[Ca^{2+}]_i$ rise (Fig. 3*B*) corresponded to the temporal course of FF (Fig. 2*C*). To partly address this question, repetitive imaging of Ca^{2+} in dendrites and soma using Calcium Orange was performed throughout the stimulation train in a separate set of young-adult neurons ($n = 6$). In these studies, relative changes in Ca^{2+} fluorescence ($\%\Delta F/F$) were measured in sequential 2 sec periods throughout the suprathreshold stimulation train. The main apical dendritic shaft was imaged in different segments along the inner ~200 μm of the dendritic tree (Fig. 5*A*). In accord with previous studies (Miyakawa et al., 1992; Regehr and Tank, 1992; Jaffe and Brown, 1994b; Schiller et al., 1995; Magee and Johnston, 1997), Ca^{2+} responses in neurons reached asymptote more rapidly in proximal regions of the apical dendrite than in the soma (Fig. 5*B*). In young-adult cells, Ca^{2+} transients in all dendritic segments combined reached maximal values after 5.3 ± 0.8

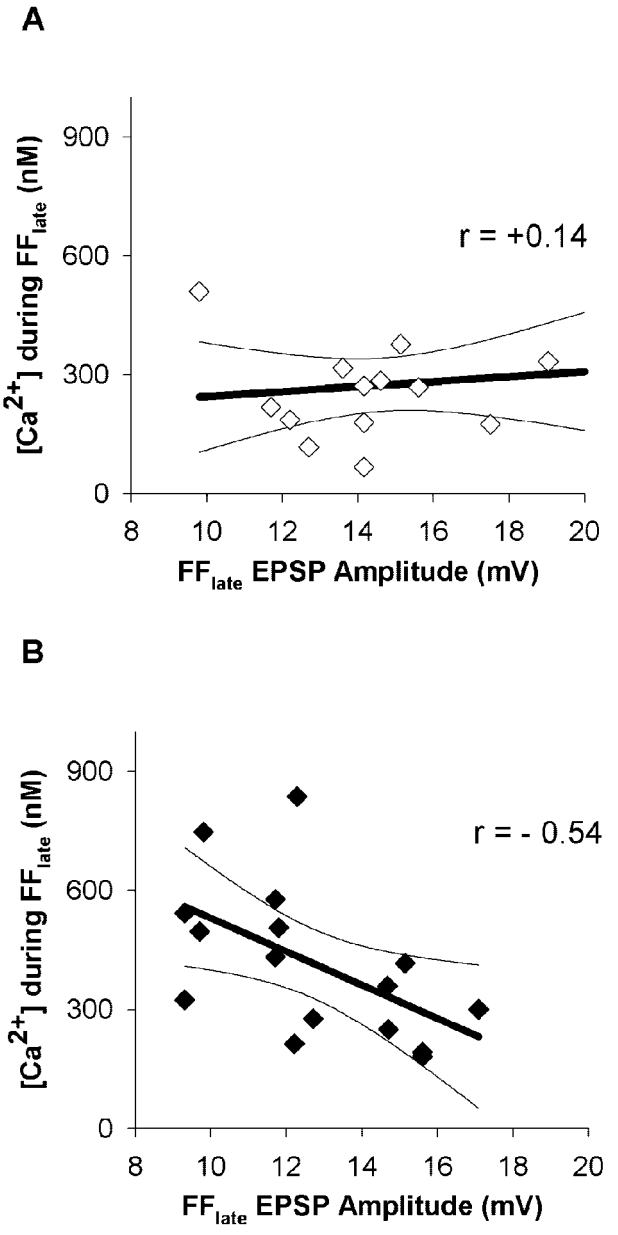

Figure 4. Correlations between mean EPSP amplitude and $[Ca^{2+}]_i$ during the last 2 sec period (FF_{late}) of the 20 sec train of suprathreshold stimulation in young-adult (*A*) and aged (*B*) neurons (*open* and *filled diamonds*, respectively). A significant inverse correlation was seen in aged neurons ($r = -0.54$; $p < 0.05$) but not in young-adult neurons. In both panels, the *thick line* shows the regression line and the *thin curved lines* delineate 95% confidence limits.

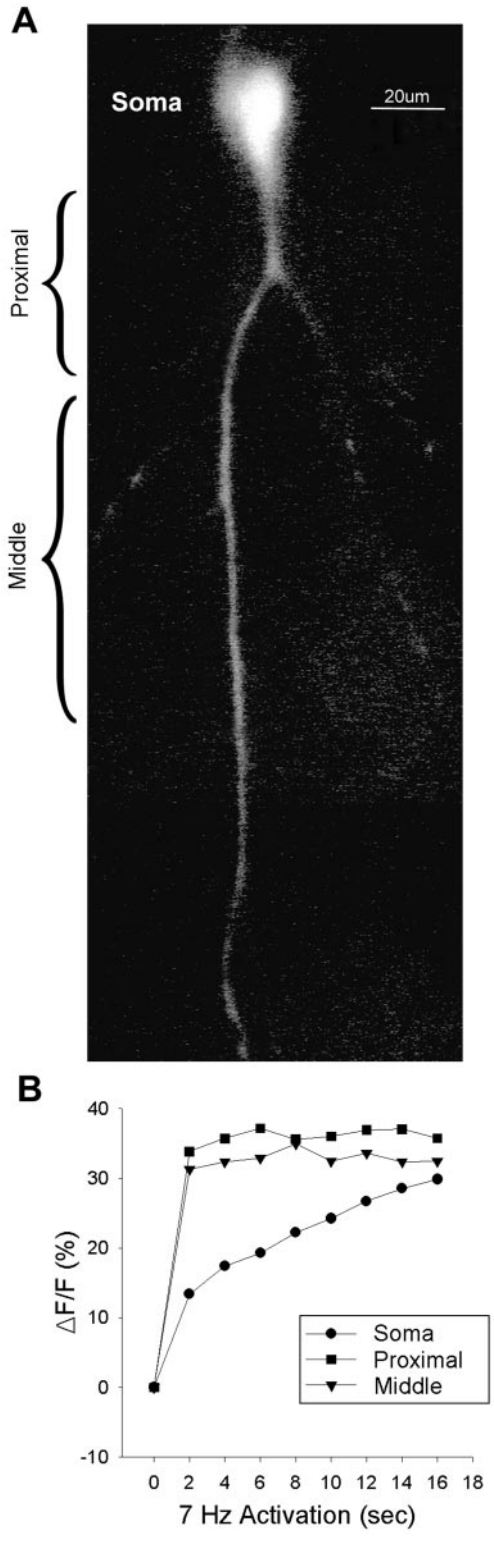

Figure 5. Representative example of Ca^{2+} imaging with the visible wavelength indicator Calcium Orange. *A*, Montage of three frames of a young-adult CA1 neuron including soma and apical dendritic shaft. *B*, Example of $\%\Delta F/F$ in different segments of a young-adult neuron in which an action potential was generated on each pulse of the 20 sec suprathreshold 7 Hz stimulation train. As reported previously by others, the most rapid Ca^{2+} changes appeared in the proximal and middle regions of the apical dendrite.

sec of stimulation, whereas somatic Ca^{2+} transients reached peak values after 13.3 ± 2.9 sec of stimulation ($p < 0.01$). Although it is not clear from these studies that aged neurons follow a similar temporal course, it seems interesting that the onset of age differences in FF (Fig. 2*C*) roughly coincided with near maximal Ca^{2+} transients in proximal dendrites, whereas the gradually increasing depression of FF in aged neurons (Fig. 2*C*) followed a temporal course more similar to that of somal accumulation of Ca^{2+} in young-adult neurons (Fig. 5*B*). However, additional studies clearly will be needed to determine whether these temporal patterns are similar in aged neurons.

Bay K8644 mimics aging effects in young-adult neurons

The highly selective L-VSCC agonist Bay K8644 substantially prolongs open time and increases the probability of opening of L-VSCCs (Fox et al., 1987; Fisher et al., 1990). Because L-VSCC density increases with aging (Thibault and Landfield, 1996) and L-VSCCs are localized primarily in postsynaptic elements (Hell et al., 1993), we tested the hypothesis that exposure to Bay K8644 in hippocampal neurons of young-adult animals would mimic the effects of aging on the AHP and on short-term synaptic plasticity. In sharp-electrode studies, the AHP is significantly prolonged and larger in CA1 neurons of aged rats (Landfield and Pitler, 1984; Kerr et al., 1989) and rabbits (Moyer et al., 1992; Disterhoft et al., 1993) and is modified by pharmacological manipulation of L-VSCCs (Mazzanti et al., 1991; Moyer et al., 1992). To confirm that a similar effect on the AHP can be detected in the whole-cell patch-clamp mode, we tested AHPs in nine aged and nine young-adult neurons (from five and five animals, respectively) under patch-clamp conditions. The AHP amplitude at 750 msec in aged neurons was −3.3 ± 0.4 mV versus −2.0 ± 0.3 mV in young-adult neurons ($p < 0.05$).

To test whether Bay K8644 could recreate this effect in young-adult neurons, we recorded from 24 neurons (from nine young-adult animals) in the CA1 region using the blind patch method (Blanton et al., 1989). Nine of these neurons were perfused with ACSF containing 0.1% DMSO alone for 15 min, and nine neurons were perfused with Bay K8644 (1 μM) for 15 min.

The effect of Bay K8644 on the AHP typically appeared between 1–5 min after the beginning of drug perfusion. However, to ensure maximal effect, cells were maintained for 15 min with Bay K8644 or DMSO alone before data acquisition was begun. In comparison with vehicle controls, Bay K8644-treated neurons displayed substantially larger AHPs (Fig. 6 and Table 2). Only cells that exhibited the same number of action potentials before and after Bay K8644 or DMSO were used for AHP analyses. Bay K8644 did not significantly affect action potential height, width, or threshold (data not shown).

Bay K8644-mediated depression of frequency facilitation

The same young-adult neurons examined for effects of Bay K8644 on the AHP were then run through repetitive stimulation protocols. In control DMSO cells, the FF of the EPSP and action potential generation were primarily maintained throughout the 20 sec subthreshold train (Fig. 7*A*). In contrast, although facilitation of the EPSP in Bay K8644-treated neurons was relatively normal in the initial seconds (slightly, but not significantly less than controls), FF decreased by the fourth second of stimulation and continued to decline throughout the train. In most Bay K8644-treated cells, action potential failure and full loss of FF

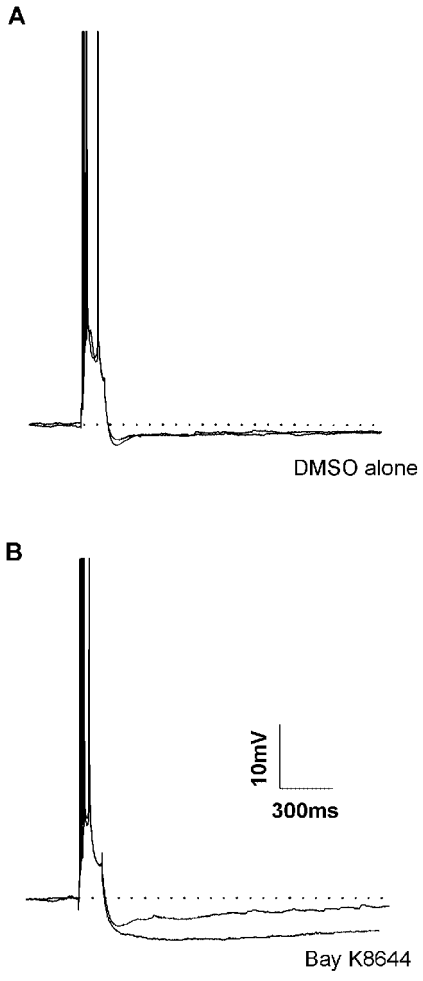

Figure 6. Representative examples of AHPs recorded in slices from young-adult animals. *A*, Superimposed AHPs were triggered from a holding potential of −60 mV at 5 min after break-in and after an additional 15 min of 0.1% DMSO bath perfusion. Three action potentials were generated on each depolarizing pulse. No differences were noted with DMSO perfusion. *B*, A similar recording paradigm and superimposition of AHP traces obtained before and after 15 min of 1 μM Bay K8644 bath perfusion (*larger trace*). The same number of action potentials was triggered before and after drug or vehicle. Bay K8644 nearly doubled the AHP (Table 2). Action potentials are truncated for illustrative purposes.

occurred by the end of the train (Fig. 7*B,C*). Two-way ANOVA revealed that Bay K8644 significantly reduced FF, and *post hoc* analyses showed that FF was significantly depressed in Bay K8644 cells over the last 16 sec of the 20 sec stimulation train ($F_{(1,16)}=15.8$; $p < 0.001$; Fig. 7*C*). A significant interaction was detected between drug treatment and stimulation ($F_{(19,16)}=5.9$; $p < 0.001$), indicating that Bay K8644 depressed EPSP facilitation more prominently with increasing stimulation duration.

In suprathreshold protocols, the initial hyperpolarization is often succeeded by a depolarization phase (see Materials and Methods). In the present study, the membrane potential was depolarized significantly more during suprathreshold activation in Bay K8644-treated cells versus controls (Fig. 7*B*; Table 2; $p < 0.001$; Tukey's test). This effect of Bay K8644 may be attributable to the greater AHP conductance (Fig. 6). Although these depolarization/hyperpolarization shifts do not generally affect FF (Pitler and Landfield, 1987), we studied an additional six Bay K8644-treated cells to control for the possibility that the larger depolarizing membrane voltage shift here might alter EPSP driving force or channel inactivation and influence EPSP depression during the 20 sec of stimulation. In these six neurons, we maintained membrane potential at approximately −70 mV throughout the stimulation train by injecting small amounts of hyperpolarizing current (Table 2). Under these conditions, Bay K8644 still significantly attenuated FF to essentially the same degree as seen without hyperpolarization (FF was 23.4 ± 3.5% for the first 2 sec of stimulation and −18.3 ± 13.6% for the last 2 sec of stimulation in membrane-stabilized Bay K8644 cells). Accordingly, the depolarization was not necessary for the substantial FF depression seen in Bay K8644. Because these six neurons were hyperpolarized only during the repetitive stimulation train, data from the Bay K8644 hyperpolarized and nonhyperpolarized cells were combined for basic electrophysiological measures, including input resistance, AHP amplitude, and stimulus input threshold ($n = 15$, Table 2).

In contrast, during the subthreshold simulation protocol ($n = 8$ Bay K8644 cells and 9 control cells), membrane potential did not exhibit a depolarization phase in either group, and neither FF nor membrane potential differed significantly between the Bay K8644 and the DMSO groups (Table 2). Thus, as with aging, repetitive action potential generation for several seconds appeared necessary for Bay K8644 to depress FF.

DISCUSSION

The present studies found that $[Ca^{2+}]_i$ was elevated in hippocampal neurons of aged versus young-adult rats during comparable degrees of synaptic and voltage-dependent activation. Concomitant intracellular recordings ruled out the possibility that differences in membrane depolarization or action potential generation could account for the age differences in $[Ca^{2+}]_i$. In addition, because our yields of aged and young-adult neurons were generally similar, as were resting parameters (Table 1), an interaction of preparation procedure with age on cell health seems unlikely to have been a major factor in the results. These conclusions are also supported by the findings that age differences in $[Ca^{2+}]_i$ were found only under a very restricted set of conditions. Together, these results strongly suggest that $[Ca^{2+}]_i$ is normally elevated in hippocampal neurons of aged animals during physiologically relevant frequencies of repetitive firing.

Relationship of $[Ca^{2+}]_i$ to short-term synaptic plasticity

Age effects on FF and on $[Ca^{2+}]_i$ were seen under essentially the same conditions, specifically during stimulation above action potential threshold and in the later phases of a repetitive activation train. Moreover, the two processes were negatively correlated across individual aged neurons, notably at the time point at which they were both altered with aging.

These observed associations between FF and $[Ca^{2+}]_i$ are consistent with the hypothesis that elevation of neuronal $[Ca^{2+}]_i$ in soma, and possibly, in dendrites, negatively regulates the amplitude of the somal EPSP during repetitive activation. Of course, correlational data alone cannot provide definitive evidence for this putative causal relationship.

Enhanced L-VSCC activity was sufficient to mimic age-related impaired plasticity

In addition to the above correlations, however, our results show that a highly selective pharmacologic intervention, the enhancement of L-VSCC activity in young-adult neurons, was sufficient to mimic essentially the full range of aging effects on the AHP and

Table 2. Neuronal parameters in patched-clamped control and Bay K8644-treated CA1 neurons

	DMSO ($n = 9$)	Bay K8644
AHP amplitude at 750 msec (mV)	−1.9 ± 0.4	−3.6 ± 0.5* ($n = 15$)
Input resistance (MΩ)	105.8 ± 14.9	91.5 ± 10.4 ($n = 15$)
Stimulation threshold (μA)	207 ± 35.3	212 ± 75.1 ($n = 15$)
Subthreshold 7 Hz stimulation		
FF_{early} (%)	91.9 ± 23.1	98.3 ± 14.4
FF_{late} (%)	66.8 ± 21.0	55.3 ± 14.5
FF_{early}, membrane potential (mV)	−70.9 ± 0.2	−71.1 ± 0.1 ($n = 8$)
FF_{late}, membrane potential (mV)	−70.6 ± 0.3	−68.7 ± 0.5 ($n = 8$)
Suprathreshold 7 Hz stimulation		
FF_{early}, membrane potential (mV)	−71.1 ± 0.5	−69.7 ± 0.4 ($n = 9$)
FF_{late}, membrane potential (mV)	−67.3 ± 0.7	−61.7 ± 0.9** ($n = 9$)
Suprathreshold 7 Hz stimulation + current injection		
FF_{early}, membrane potential (mV)	N/A	−71.6 ± 0.8 ($n = 6$)
FF_{late}, membrane potential (mV)	N/A	−71.1 ± 0.3 ($n = 6$)

All values are mean ± SEM. *$p < 0.05$; **$p < 0.001$ for DMSO versus Bay K8644 effect. Values for FF or membrane potential are 2 sec averages obtained during the first 2 sec and last 2 sec periods of a 20 sec train of 7 Hz of synaptic activation. N/A, Not applicable.

on FF. Bay K8644 dramatically accelerated the depression of FF in young-adult CA1 neurons (Fig. 7*C*), with a temporal course roughly analogous to the depression seen in aged neurons (Fig. 2*C*). Intriguingly, Bay K8644 was effective in impairing FF only under the same conditions as those under which aging impaired FF (i.e., with suprathreshold repetitive synaptic stimulation lasting at least several seconds) (Fig. 7*C*). This pattern of effects of Bay K8644 on AHP enhancement and FF depression was essentially identical to that of aging. Thus, the present results suggest that the increase in the L-VSCC pathway in CA1 neurons that occurs with aging (Thibault and Landfield, 1996) may be sufficient to impair aspects of short-term plasticity.

Sources of elevated $[Ca^{2+}]_i$

The finding that the age-related increase in $[Ca^{2+}]_i$ responses is seen only during repetitive action potentials, presumably propagated throughout the soma and dendrites (Miyakawa et al., 1992; Schiller et al., 1995; Johnston et al., 1999), indicates that this aging effect depends on activation of voltage-dependent channels. However, although Bay K8644 increases $[Ca^{2+}]_i$ responses during repetitive activation (Regehr and Tank, 1992), the action potential dependence of the aging effect does not of course demonstrate that the L-VSCC is the primary source of elevated $[Ca^{2+}]_i$ in aged neurons. Voltage-dependent elevation of Ca^{2+} also occurs via both NMDA receptors (Regehr et al., 1989; Alford et al., 1993; Perkel et al., 1993; Schiller et al., 1998; Yuste et al., 1999) and other VSCCs (Miyakawa et al., 1992; Brown and Jaffe, 1994; Markram and Sakmann, 1994; Elliott et al., 1995; Magee and Johnston, 1995; Randall and Tsien, 1995). Moreover, multiple Ca^{2+}- and receptor-mediated pathways, including the L-VSCC, trigger Ca^{2+} release from intracellular stores (Jaffe and Brown, 1994a; Llano et al., 1994; Gruol et al., 1996; Emptage et al., 1999; Murchison and Griffith, 1999; Nakamura et al., 1999). Several of these alternative pathways, as well as buffering/clearance mechanisms, also are altered with age (Ito et al., 1994; Michaelis et al., 1996; Murchison and Griffith, 1999) (for review, see Thibault et al., 1998; Verkhratsky and Toescu, 1998; Griffith et al., 2000) and could contribute to overall Ca^{2+} dysregulation and/or alterations in Ca^{2+} microdomains. Thus, additional studies will be needed to unravel the complex interactions and relative contributions among multiple Ca^{2+} regulatory processes in aging. Nevertheless, the present data suggest that enhanced L-VSCC activity plays an important role in impaired plasticity and, very likely, in the elevation of $[Ca^{2+}]_i$.

Presynaptic versus postsynaptic impairment

Presynaptic fatigue during repetitive activation can depress transmission (Rosenmund and Stevens, 1996; Zucker, 1996; Hagler and Goda, 2001) (see Materials and Methods). However, the depression of FF during suprathreshold stimulation seen here does not seem to be accounted for by presynaptic factors. That is, whether with aging or Bay K8644, much less FF depression developed during subthreshold (Fig. 1*C*, Table 2) compared with suprathreshold activation (Figs. 2*C*, 7*C*). Although fewer presynaptic fibers are activated in a subthreshold protocol, each activated fiber in either protocol should have been activated by the same number of presynaptic action potentials. Therefore, the primary distinction between the subthreshold and suprathreshold protocols apparently was the generation of postsynaptic action potentials. In addition, enhancement of L-VSCCs by Bay K8644 induced almost complete depression of FF (Fig. 7*C*) and localization of L-VSCCs is almost completely postsynaptic (Hell et al., 1993). The Schaffer collateral/commissural presynaptic fibers activated in these studies are also able to sustain minutes of 10 Hz activation without major synaptic vesicle depletion (Applegate and Landfield, 1988). Therefore, postsynaptic factors (e.g., action potentials and the conductances they activate, L-VSCC activity) appeared to provide the basis for FF depression in suprathreshold protocols.

Hippocampal FF has been found to change with aging in multiple studies (Landfield et al., 1978, 1986; Applegate and Landfield, 1988; Rosenzweig et al., 1997; Ouanounou et al., 1999), but it was previously not known whether presynaptic or postsynaptic factors underlie the FF deficit, nor under which specific conditions a deficit is seen. However, the aforementioned evidence clearly suggests that postsynaptic mechanisms play the primary role in age-related impairment of hippocampal short-term synaptic plasticity.

Mechanisms of impaired FF

One postsynaptic mechanism that could link high $[Ca^{2+}]_i$ and/or elevated L-VSCC activity to impaired FF is excessive activation

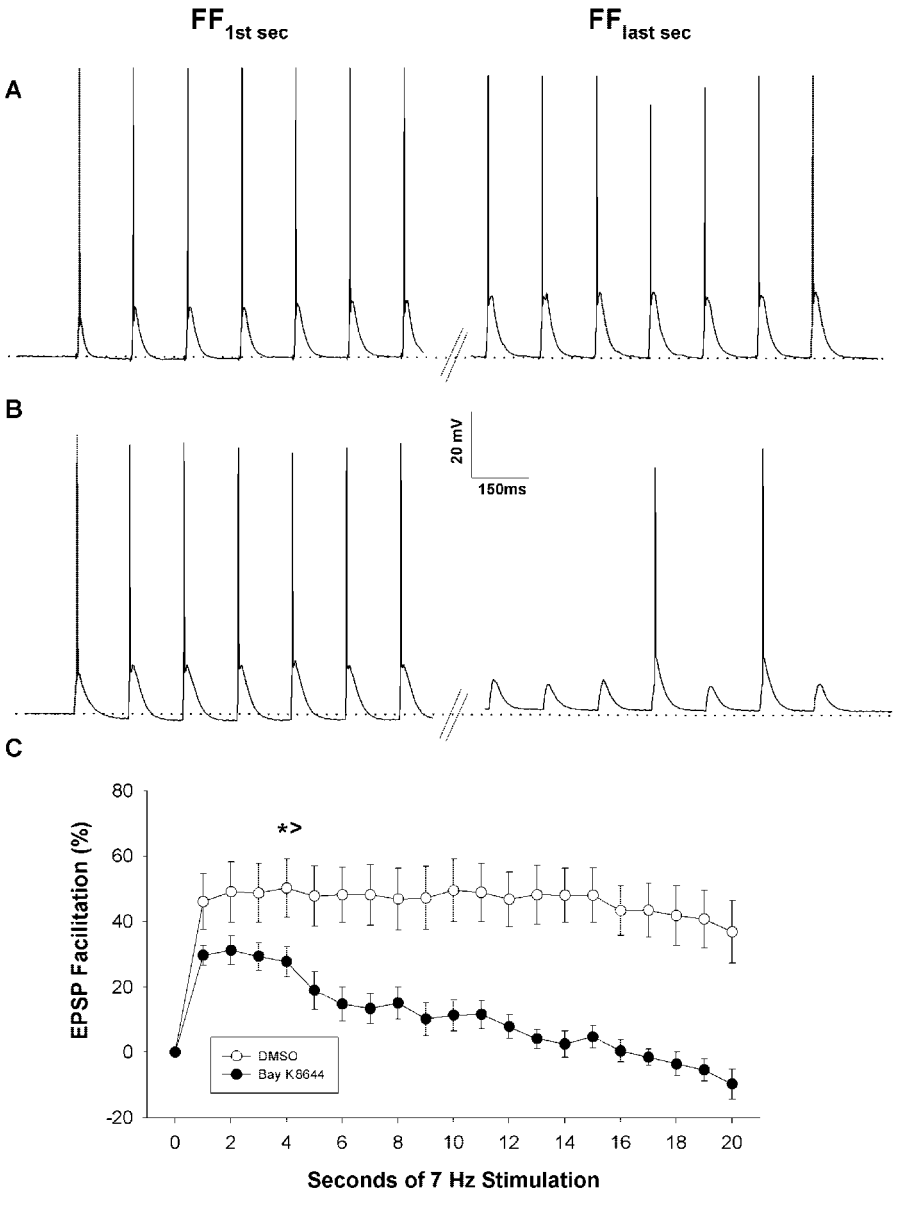

Figure 7. Representative voltage traces of the first and last seconds of repetitive FF stimulation in young-adult neurons recorded with or without Bay K8644 exposure. *A*, After 15 min of exposure to DMSO alone, EPSP facilitation was well-maintained throughout the duration of the train. *B*, In contrast, after 15 min of Bay K8644 exposure, strong EPSP depression was seen by the end of the stimulation protocol along with significant membrane depolarization (Table 2). To offset the Bay K8644-induced depolarization during FF, some cells were hyperpolarized during the stimulation train. Despite hyperpolarization, Bay K8644 still significantly depressed FF (data not shown). *C*, Mean ± SEM for EPSP frequency facilitation during 7 Hz of stimulation in DMSO control neurons or Bay K8644-treated neurons. Bay K8644 significantly depressed FF after the fourth second of stimulation compared with DMSO control conditions. *> Bay K8644 and vehicle significantly different ($p < 0.05$) at this point and each point thereafter.

of Ca^{2+}-dependent K^+ or Cl^- "shunting" conductances. It has been shown, for example, that the increased hippocampal AHP with aging results in greater accommodation and spike failure (Moyer et al., 1992; Disterhoft et al., 1993). However, the shunting effect of a single AHP (Fig. 6) or of a single action potential (Häusser et al., 2001) apparently is not sufficient to counteract EPSP facilitation, because several seconds of activation were required for depression (Figs. 2*C*, 7*C*). Therefore, some threshold level of Ca^{2+} accumulation induced by repetitive action potentials in soma or dendrites might be required to activate relevant shunting conductances in dendrites and soma (Sah and Bekkers, 1996; Schwindt and Crill, 1997; Johnston et al., 1999). Alternatively, elevated $[Ca^{2+}]_i$ could impair FF by inactivating NMDA receptors (Rosenmund et al., 1995; Tong et al., 1995) or triggering Ca^{2+} signaling pathways that enhance concurrent LTD (Foster and Norris, 1997; Norris et al., 1998), among other possibilities.

Functional implications

The present results provide evidence that hippocampal $[Ca^{2+}]_i$ elevation during physiological frequencies (7 Hz) of repetitive action potentials is relatively greater in aged neurons compared with young-adult neurons. In turn, this $[Ca^{2+}]_i$ elevation was closely correlated with depression of FF. Moreover, enhanced L-VSCC activity, as is present with aging (Thibault and Landfield, 1996), directly suppressed FF at 7 Hz. Firing frequencies in the 5–10 Hz range are often seen in hippocampal neurons *in vivo*, notably during theta rhythms (Foster et al., 1987; Mizumori et al., 1990) that are closely correlated with attention, cognition, and memory processing (for review, see Landfield and Thibault, 2001). Thus, it can be inferred that $[Ca^{2+}]_i$ is likely elevated and FF is impaired in aged hippocampal neurons during the theta frequencies associated with cognitive processing.

FF is a prominent form of short-term plasticity that importantly regulates throughput in multisynaptic systems (Andersen and Lomo, 1970) and has been linked to both LTP induction (Rosenzweig et al., 1997) and cognitive function (Landfield, 1988). Therefore, impaired FF during theta rhythms implies that in aged brain neurons, the extent of neuronal activation, LTP induction, and, as a corollary, memory formation, might well be reduced.

Moreover, in addition to functional impairment, the chronic elevation of $[Ca^{2+}]_i$ during physiological activity could erode neuronal structural integrity and set the stage for eventual neurodegenerative disease.

REFERENCES

Alford S, Frenguelli BG, Schofield JG, Collingridge L (1993) Characterization of Ca^{2+} signals induced in hippocampal CA1 neurons by the synaptic activation of NMDA receptors. J Physiol (Lond) 469:693–716.

Alger BE, Teyler TJ (1978) Potassium and short-term response plasticity in the hippocampal slice. Brain Res 159:239–242.

Andersen P, Lomo T (1970) Mode of control of hippocampal pyramidal cell discharges. In: The neural control of behavior (Whalen RE, Thompson RF, Verzeano M, Weinberger NM, eds), pp 3–25. New York: Academic.

Applegate MD, Landfield PW (1988) Synaptic vesicle redistribution during hippocampal frequency potentiation and depression in young and aged rats. J Neurosci 8:1096–1111.

Bach ME, Barad M, Son H, Zhuo M, Lu YF, Shih R, Mansuy I, Hawkins RD, Kandel ER (1999) Age-related defects in spatial memory are correlated with defects in the late phase of hippocampal long-term potentiation in vitro and are attenuated by drugs that enhance the cAMP signaling pathway. Proc Natl Acad Sci USA 96:5280–5285.

Barnes CA (1979) Memory deficits associated with senescence: a behavioral and neurophysiological study in the rat. J Comp Physiol Psychol 93:74–104.

Barnes CA (1994) Normal aging: regionally specific changes in hippocampal synaptic transmission. Trends Neurosci 17:8–13.

Barnes CA, McNaughton BL (1980) Physiological compensation for loss of afferent synapses in rat hippocampal granule cells during senescence. J Physiol (Lond) 309:473–485.

Barnes CA, Rao G, Shen J (1997) Age-related decrease in the *N*-methyl-D-aspartateR-mediated excitatory postsynaptic potential in hippocampal region CA1. Neurobiol Aging 18:445–452.

Blanton MG, Lo Turco JJ, Kriegstein AR (1989) Whole cell recording from neurons in slices of reptilian and mammalian cortex. J Neurosci Methods 30:203–210.

Brown TH, Jaffe DB (1994) Calcium imaging in hippocampal neurons using confocal microscopy. Ann NY Acad Sci 747:313–324.

Campbell LW, Hao S-Y, Thibault O, Blalock EM, Landfield PW (1996) Aging changes in voltage-gated calcium currents in hippocampal CA1 neurons. J Neurosci 16:6286–6295.

Creager R, Dunwiddie T, Lynch G (1980) Paired-pulse and frequency facilitation in the CA1 region of the in vitro rat hippocampus. J Physiol (Lond) 299:409–424.

Davies CH, Collingridge GL (1996) Regulation of EPSPs by the synaptic activation of $GABA_B$ autoreceptors in rat hippocampus. J Physiol (Lond) 496:451–470.

Deyo RA, Straube KT, Disterhoft JF (1989) Nimodipine facilitates associative learning in aging rabbits. Science 243:809–811.

Disterhoft JF, Moyer JR, Thompson LT, Kowalska M (1993) Functional aspects of calcium-channel modulation. Clin Neuropharmacol 16:S12–S24.

Disterhoft JF, Thompson LT, Moyer JR, Mogul DJ (1996) Calcium-dependent afterhyperpolarization and learning in young and aging hippocampus. Life Sci 59:413–420.

Elliott EM, Malouf AT, Catterall WA (1995) Role of calcium channel subtypes in calcium transients in hippocampal CA3 neurons. J Neurosci 15:6433–6444.

Emptage N, Bliss TVP, Fine A (1999) Single synaptic events evoke NMDA receptor-mediated release of calcium from internal stores in hippocampal dendritic spines. Neuron 22:115–124.

Fisher RE, Gray R, Johnston D (1990) Properties and distribution of single voltage-gated calcium channels in adult hippocampal neurons. J Neurophysiol 64:91–104.

Foster TC, Norris CM (1997) Age-associated changes in Ca^{2+}-dependent processes: relationship to hippocampal synaptic plasticity. Hippocampus 7:602–612.

Foster TC, Christian EP, Hampson RE, Campbell KA, Deadwyler SA (1987) Sequential dependencies regulate sensory evoked responses of single units in the rat hippocampus. Brain Res 408:86–96.

Fox AP, Nowycky MC, Tsien RW (1987) Kinetics and pharmacological properties distinguishing three types of calcium currents in chick sensory neurons. J Physiol (Lond) 394:149–172.

Gibson GE, Peterson C (1987) Calcium and the aging nervous system. Neurobiol Aging 8:329–343.

Griffith WH, Jasek MC, Bain SH, Murchison D (2000) Modification of ion channels and calcium homeostasis of basal forebrain neurons during aging. Behav Brain Res 115:219–233.

Gruol DL, Netzeband JG, Parsons KL (1996) Ca^{2+} signaling pathways linked to glutamate receptor activation in the somatic and dendritic regions of cultured cerebellar Purkinje neurons. J Neurophysiol 76:3325–3340.

Grynkiewicz G, Poenie M, Tsien RY (1985) A new generation of Ca^{2+} indicators with greatly improved fluorescence properties. J Biol Chem 260:3440–3450.

Hagler DJ, Goda Y (2001) Properties of synchronous and asynchronous release during pulse train depression in cultured neurons. J Neurophysiol 85:2324–2334.

Häusser M, Major G, Stuart GJ (2001) Differential shunting of EPSPs by action potentials. Science 291:138–141.

Hell JW, Westenbroek RE, Warner C, Ahlijanian MK, Prystay W, Gilbert MM, Snutch TP, Catterall WA (1993) Identification and differential subcellular localization of the neuronal class C and class D L-type calcium channel 1 subunits. J Cell Biol 123:949–962.

Ito E, Oka K, Etcheberrigaray R, Nelson TJ, McPhie DL, Tofel-Grehl B, Gibson GE, Alkon DL (1994) Internal Ca^{2+} mobilization is altered in fibroblasts from patients with Alzheimer disease. Proc Natl Acad Sci USA 91:534–538.

Jaffe DB, Brown TH (1994a) Metabotrotopic glutamate receptor activation induces calcium waves within hippocampal dendrites. J Neurophysiol 72:471–474.

Jaffe DB, Brown TH (1994b) Confocal imaging of dendritic Ca transients in hippocampal brain slices during simultaneous current- and voltage-clamp recording. Microsc Res Tech 29:279–289.

Johnston D, Hoffman DA, Colbert CM, Magee JC (1999) Regulation of back-propagating action potentials in hippocampal neurons. Curr Opin Neurobiol 9:288–292.

Kerr DS, Campbell LW, Hao S-Y, Landfield PW (1989) Corticosteroid modulation of hippocampal potentials: increased effect with aging. Science 245:1505–1509.

Khachaturian ZS (1984) Towards theories of brain aging. In: Handbook of studies on psychiatry and old age (Kay D, Burrows GD, eds), pp 7–30. Amsterdam: Elsevier.

Khachaturian ZS (1989) The role of calcium regulation in brain aging: reexamination of a hypothesis. Aging 1:17–34.

Kirischuk S, Verkhratsky A (1996) $[Ca^{2+}]_i$ recordings from neural cells in acutely isolated cerebellar slices employing differential loading of the membrane-permeant form of calcium indicator fura-2. Pflügers Arch 431:977–983.

Kreitzer AC, Gee KR, Archer EA, Regehr WG (2000) Monitoring presynaptic calcium dynamics in projection fibers by in vivo loading of a novel calcium indicator. Neuron 27:25–32.

Landfield PW (1988) Hippocampal neurobiological mechanisms of age-related memory dysfunction. Neurobiol Aging 9:571–579.

Landfield PW, Pitler TA (1984) Prolonged Ca^{2+}-dependent afterhyperpolarizations in hippocampal neurons of aged rats. Science 226:1089–1092.

Landfield PW, Thibault O (2001) A neuroholographic model of memory: theta rhythms, facilitation, and calcium channels. In: Memory consolidation: essays in honor of James L. McGaugh (Gold PE, Greenough WT, eds), pp 295–320. Washington, DC: American Psychological Association.

Landfield PW, McGaugh JL, Lynch G (1978) Impaired synaptic potentiation processes in the hippocampus of aged, memory-deficient rats. Brain Res 150:85–101.

Landfield PW, Pitler TA, Applegate MD (1986) The effects of high Mg^{2+} to Ca^{2+} ratios on frequency potentiation in hippocampal slices of young and aged animals. J Neurophysiol 56:797–811.

Landfield PW, Campbell LW, Hao S-Y, Kerr DS (1989) Aging-related increases in voltage-sensitive, inactivating calcium currents in rat hippocampus. Implications for mechanisms of brain aging and Alzheimer's disease. Ann NY Acad Sci 568:95–105.

Llano I, DiPolo R, Marty A (1994) Calcium-induced calcium release in cerebellar Purkinje cells. Neuron 12:663–673.

Madison DV, Nicoll RA (1984) Control of the repetitive discharge of rat CA1 pyramidal neurones in vitro. J Physiol (Lond) 354:319–331.

Magee JC, Johnston D (1995) Synaptic activation of voltage-gated channels in the dendrites of hippocampal pyramidal neurons. Science 268:301–304.

Magee JC, Johnston D (1997) A synaptically controlled, associative signal for Hebbian plasticity in hippocampal neurons. Science 275:209–213.

Magleby KL (1987) Short-term changes in synaptic efficacy. In: Synaptic function (Edelman GM, Gall WE, Cowan WM, eds), pp 21–56. New York: Wiley.

Markram H, Sakmann B (1994) Calcium transients in dendrites of neocortical neurons evoked by single subthreshold excitatory postsynaptic potentials via low-voltage-activated calcium channels. Proc Natl Acad Sci USA 91:5207–5211.

Mazzanti ML, Thibault O, Landfield PW (1991) Dihydropyridine modulation of normal hippocampal physiology in young and aged rats. Neurosci Res Commun 9:117–125.

McCarren M, Alger BE (1985) Use-dependent depression of IPSPs in rat hippocampal pyramidal cells in vitro. J Neurophysiol 53:557–571.

Michaelis ML, Johe K, Kitos TE (1984) Age-dependent alterations in synaptic membrane systems for Ca^{2+} regulation. Mech Aging Dev 25:215–225.

Michaelis M, Bigelow DJ, Schöneich C, Williams TD, Ramonda L, Yin D, Hühmer AFR, Yao Y, Gao J, Squier TC (1996) Decreased plasma membrane calcium transport activity in aging brain. Life Sci 59:405–412.

Miyakawa H, Ross WN, Jaffe D, Callaway JC, Lasser-Ross N, Lisman JE, Johnston D (1992) Synaptically activated increases in Ca^{2+} concentration in hippocampal CA1 pyramidal cells are primarily due to voltage-gated Ca^{2+} channels. Neuron 9:1163–1173.

Mizumori SJ, Barnes CA, McNaughton BL (1990) Behavioral correlates of theta-on and theta-off cells recorded from hippocampal formation of mature young and aged rats. Exp Brain Res 80:365–373.

Moore CI, Browning MD, Rose GM (1993) Hippocampal plasticity induced by primed burst but not long-term potentiation stimulation is impaired in area CA1 of aged Fischer 344 rats. Hippocampus 3:57–66.

Moyer Jr JR, Brown TH (1998) Methods for whole-cell recording from visually preselected neurons of perirhinal cortex in brain slices from young and aging rats. J Neurosci Methods 86:35–54.

Moyer JR, Thompson LT, Black JP, Disterhoft JF (1992) Nimodipine increases excitability of rabbit CA1 pyramidal neurons in an age- and concentration-dependent manner. J Neurophysiol 68:2100–2109.

Murchison D, Griffith WH (1998) Increased calcium buffering in basal forebrain neurons during aging. J Neurophysiol 80:350–364.

Murchison D, Griffith WH (1999) Age-related alterations in caffeine-sensitive calcium stores and mitochondrial buffering in rat basal forebrain. Cell Calcium 25:439–452.

Nakamura T, Barbara J-G, Nakamura K, Ross WN (1999) Synergic release of Ca^{2+} from IP3-sensitive stores evoked by synaptic activation of mGluRs paired with backpropagating action potentials. Neuron 24:727–737.

Newberry NR, Nicoll RA (1984) A bicuculline-resistant inhibitory postsynaptic potential in rat hippocampal pyramidal cells in vitro. J Physiol (Lond) 348:239–254.

Norris CM, Korol DL, Foster TC (1996) Increased susceptibility to induction of long-term depression and long-term potentiation reversal during aging. J Neurosci 16:5382–5392.

Norris CM, Halpain S, Foster TC (1998) Reversal of age-related alterations in synaptic plasticity by blockade of L-type Ca^{2+} channels. J Neurosci 18:3171–3179.

Ouanounou A, Zhang L, Charlton MP, Carlen PL (1999) Differential modulation of synaptic transmission by calcium chelators in young and aged hippocampal CA1 neurons: evidence for altered calcium homeostasis in aging. J Neurosci 19:906–915.

Perkel DJ, Petrozzino JJ, Nicoll RA, Connor JA (1993) The role of Ca entry via synaptically activated NMDA receptors in the induction of long-term potentiation. Neuron 11:817–823.

Peterson C, Nicholls DG, Gibson GE (1985) Subsynaptosomal distribution of calcium during aging and 3,4-diaminopyridine treatment. Neurobiol Aging 6:297–304.

Pitler TA, Landfield PW (1987) Postsynaptic membrane shifts during frequency potentiation of the hippocampal EPSP. J Neurophysiol 58:866–882.

Porter NM, Thibault O, Thibault V, Chen KC, Landfield PW (1997) Calcium channel density and hippocampal cell death with age in long-term culture. J Neurosci 17:5629–5639.

Potier B, Lamour Y, Dutar P (1993) Age-related alterations in the properties of hippocampal pyramidal neurons among rat strains. Neurobiol Aging 14:17–25.

Randall A, Tsien RW (1995) Pharmacological dissection of multiple types of Ca^{2+} channel currents in rat cerebellar granule neurons. J Neurosci 15:2995–3012.

Regehr WG, Tank DW (1992) Calcium concentration dynamics produced by synaptic activation of CA1 hippocampal pyramidal cells. J Neurosci 12:4202–4223.

Regehr WG, Connor JA, Tank DW (1989) Optical imaging of calcium accumulation in hippocampal pyramidal cells during synaptic activation. Nature 341:533–536.

Rosenmund C, Stevens CF (1996) Definition of the readily releasable pool of vesicles at hippocampal synapses. Neuron 16:1197–1207.

Rosenmund C, Feltz A, Westbrook GL (1995) Calcium-dependent inactivation of synaptic NMDA receptors in hippocampal neurons. J Neurophysiol 74:427–430.

Rosenzweig ES, Rao G, McNaughton BL, Barnes CA (1997) Role of temporal summation in age-related long-term potentiation-induction deficits. Hippocampus 7:549–558.

Sah P, Bekkers JM (1996) Apical dendritic location of slow afterhyperpolarization current in hippocampal pyramidal neurons: implications for the integration of long-term potentiation. J Neurosci 16:4537–4542.

Schiller J, Helmchen F, Sakmann B (1995) Spatial profile of dendritic calcium transients evoked by action potentials in rat neocortical pyramidal neurons. J Physiol (Lond) 487:583–600.

Schiller J, Schiller Y, Clapham DE (1998) NMDA receptors amplify calcium influx into dendritic spines during associative pre- and postsynaptic activation. Nat Neurosci 1:114–118.

Schwindt PC, Crill WE (1997) Modification of current transmitted from apical dendrite to soma by blockade of voltage- and Ca^{2+}-dependent conductances in rat neocortical pyramidal neurons. J Neurophysiol 78:187–198.

Scriabine A, Schuurman T, Traber J (1989) Pharmacological basis for the use of nimodipine in central nervous system disorders. FASEB J 3:1799–1806.

Shankar S, Teyler TJ, Robbins N (1998) Aging differentially alters forms of long-term potentiation in rat hippocampal area CA1. J Neurophysiol 79:334–341.

Storm JF (1990) Potassium currents in hippocampal pyramidal cells. Prog Brain Res 83:161–187.

Thibault O, Landfield PW (1996) Increase in single L-type calcium channels in hippocampal neurons during aging. Science 272:1017–1020.

Thibault O, Porter NM, Chen K-C, Blalock EM, Kaminker PG, Clodfelter GV, Brewer LD, Landfield PW (1998) Calcium dysregulation in neuronal aging and Alzheimer's disease: history and new directions. Cell Calcium 24:417–433.

Tong G, Sheperd D, Jahr CE (1995) Synaptic desensitization of NMDA receptors by calcineurin. Science 267:1510–1512.

Verkhratsky A, Toescu EC (1998) Calcium and neuronal ageing. Trends Neurosci 2:12–17.

Yuste R, Majeweski A, Cash SS, Denk W (1999) Mechanisms of calcium influx into hippocampal spines: heterogeneity among spines, coincidence detection by NMDA receptors, and optical quantal analysis. J Neurosci 19:1976–1987.

Zucker ES (1996) Exocytosis: a molecular and physiological perspective. Neuron 17:1049–1055.